NJC

This article can be cited before page numbers have been issued, to do this please use: S. Cheng, N. Shang, X. Zhou, C. Feng, S. Gao, C. Wang and Z. Wang, *New J. Chem.*, 2017, DOI: 10.1039/C7NJ00442G.

Volume 40 | Number 1 | January 2016 | Pages 1–846

NJC

New Journal of Chemistry
www.rsc.org/njc

A journal for new directions in chemistry

ISSN 1144-0546

ROYAL SOCIETY OF CHEMISTRY

PAPER
Jason B. Benedict *et al.*
The role of atropisomers on the photo-reactivity and fatigue of diarylethene-based metal–organic frameworks

ROYAL SOCIETY OF CHEMISTRY

rsc.li/njc

View Article Online
DOI: 10.1039/C7NJ00442G

Journal Name

ARTICLE

High catalytic activity of bimetallic AgPd alloy supported on UiO-66 derived porous carbon for transfer hydrogenation of nitroarenes using formic acid-formate as hydrogen source

Received 00th January 20xx,
Accepted 00th January 20xx

DOI: 10.1039/x0xx00000x

www.rsc.org/

Saisai Cheng, Ningzhao Shang, Xin Zhou, Cheng Feng*, Shutao Gao, Chun Wang*, Zhi Wang

College of Science, Hebei Agricultural University, Baoding 071001, China

Bimetallic AgPd nanoparticles anchored on metal-organic framework (UiO-66) derived *N*-doped porous carbon (NPC-UiO-66) was fabricated and used as the catalyst for the catalytic transfer hydrogenation of nitroarenes using formic acid-formate as hydrogen source. The results demonstrated that Ag_1Pd_9@NPC-UiO-66 composite exhibited extraordinary catalytic activity toward the hydrogenation of nitroarenes to anilines at room temperature. A series of substituted nitroarenes were successfully converted to the corresponding anilines in high yields under ambient conditions with other reducible groups remaining intact. The superior catalytic performance of the prepared catalyst can be attributed to the synergistic effect between the highly dispersed AgPd nanoparticles and the unique structure of NPC-UiO-66 support, as well as the high adsorption ability of the catalyst for the nitroarenes.

1. Introduction

Aromatic amines, especially with the functionalized groups, are known as major feedstock, ubiquitous building blocks for the manufacture of functional polymers, pharmaceuticals, agrochemicals, dyes, fine chemicals, and more.[1] The most commonly employed method for the fabrication of aromatic anilines is the reduction of corresponding nitroarenes. However, the traditional noncatalytic reduction approach requires stoichiometric reducing agents (such as Zn, Fe, Sn and metal sulfides) that produce large amount of waste acids and residues, which result in serious environmental pollution problems.[2]

In contrast, the catalytic hydrogenation of nitro compounds with the heterogeneous or homogeneous transition-metal catalysts is a more efficient, highly selective and environmental-friendly process.[3] Catalytic reduction with molecular hydrogen (H_2) obviously represents an attractive, more atom-economic alternative.[4] However, the reduction by H_2 is generally performed at high temperature and high pressure. Moreover, H_2 is flammable, potentially dangerous and requires special equipment for production, transportation and storage. Recently, an alternative to reduction by H_2, catalytic transfer hydrogenation (CTH)[5] of nitro compounds has attracted considerable attention in which hydrogen is replaced by a hydrogen donor, such as formic acid (FA),[6] hydrazine,[7] ammonia borane[8] and sodium borohydride.[9] The catalytic transfer hydrogenation can be performed under mild conditions (e.g. atmospheric pressure, room temperature), which represents a more cost-efficient and greener approach for the preparation of aryl amines. Among the hydrogen donor used in CTH, exploiting FA as a promising hydrogen source has received considerable interest due to its properties of non-toxicity, high energy density, excellent stability. Moreover, FA is one of the major by-products in biomass processing. So far, FA has been used as hydrogen source in the catalytic transfer hydrogenation of α-methylbenzyl alcohol,[10] fructose to γ-valerolactone,[11] alkene[12] and nitro compounds.[13] For example, Beller et al.[14] reported that trinuclear Mo_3S_4 hydrides functionalized with diphosphane ligands are efficient catalysts for the CTH of nitroarenes to the corresponding anilines at 70 ^oC using formic acid as the hydrogen donor. Rajenahally et al.[15] fabricated Fe_2O_3/NGr@C-based nano-materials and used for the CTH of nitroarenes to anilines in the presence of FA and triethylamine, the reaction was performed at 120 ^oC for 20−24 h. Cao et al.[13] reported an approach for the target-specific transformation of nitro compounds employing FA as the hydrogen source. The reactions were catalyzed by supported Au catalyst at 60 ^oC with toluene as the reaction solvent. Despite recent progress, the reported catalytic systems still have one or more shortcomings, such as toxic solvent, harsh reaction conditions and high catalyst dosage are required. Therefore, exploring highly active heterogeneous catalysts for reduction of nitroarenes is highly desirable.

The synergetic interaction between metal nanoparticles and support plays an important role for the catalytic performance of a heterogeneous catalyst.[16] Recently, metal-organic frameworks (MOFs)[17, 18] have attracted intense interest due to the advantage of

View Article Online
DOI: 10.1039/C7NJ00442G

high surface area, permanent nanoscale porosity, fascinating diverse structures, topologies, and uniform structured cavities. MOFs have been considered as ideal sacrificial templates to afford porous carbons via facile pyrolysis.[19, 20] MOF-derived porous carbons possess great merits, such as high surface area, tailorable structure and porosity. So far, MOF-derived porous carbon supported metal nanoparticles catalysts have been used to catalyze Suzuki coupling reaction,[21] reduction of nitro compounds,[22] catalytic hydrogen production reaction,[23] oxygen reduction reaction[24] and so on. Nevertheless, the applications of MOFs-derived nanoporous carbons as catalyst carriers are still in its infancy.

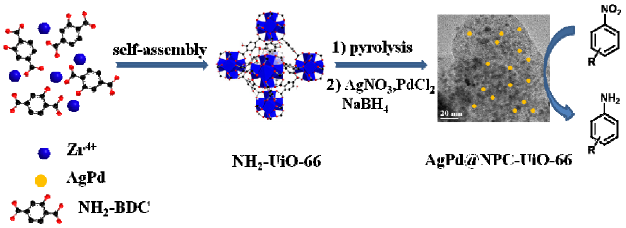

Scheme 1. Schematic illustration of the preparation process of the AgPd@NPC-UiO-66 catalyst.

UiO-66 is a Zr-based MOF with tunable pore size, high specific surface area, high thermal and chemical stability,[25] which have found widely applications in different fields.[26-28] UiO-66 might be an ideal precursor to fabricate porous carbons. To explore the application potential of MOF-derived porous carbon and investigate the effect of the porous structure on the dispersion of metal nanoparticles, herein, *N*-doped porous carbon (NPC-UiO-66) was fabricated by one-step direct carbonization of UiO-66 without using any additional carbon and nitrogen precursors. AgPd nanoparticles (NPs) were immobilized on NPC-UiO-66 by an impregnation method coupled with subsequent reduction with $NaBH_4$ (Scheme 1). To evaluate its catalytic performance, the AgPd@NPC-UiO-66 was used as catalyst for the catalytic transfer hydrogenation of nitro-compound employing FA and ammonium formate (AF) as the hydrogen source. The results demonstrated that Ag_1Pd_9@NPC-UiO-66 composite exhibited extraordinary catalytic activity and toward the reduction of nitroarenes into anilines.

2. Experimental

2.1 Chemicals

2-Amino-1,4-benzenedicarboxylic acid (NH_2-BDC), 1,4-benzenedicarboxylic acid (BDC), titanium isopropoxide (TOPT), zirconium chloride ($ZrCl_4$), zirconyl chloride octahydrate ($ZrOCl_2 \cdot 8H_2O$), aluminum chloride hexahydrate ($AlCl_3 \cdot 6H_2O$), palladium (II) chloride ($PdCl_2$, AR), sodium borohydride ($NaBH_4$, 96%) and all of the nitro compounds were obtained from Aladdin Chemicals Co Ltd. (Shanghai, China). *N,N*-Dimethylformamide (DMF), toluence, methanol, ethyl acetate, hydrochloric acid (HCl, 37%), concentrated sulphuric acid (H_2SO_4, 98%), oleic acid (OA) and ammonium hydroxide solution (NH_4OH) were obtained from Chengxin Chemical Reagents Company (Baoding, China). Silver nitrate ($AgNO_3$, AR), formic acid (HCOOH, 88%) and ammonium formate were purchased from Huaxin Co., Ltd. (Baoding, China). All materials were used as received without further purification.

2.2 Characterizations

X-ray photoelectron spectroscopy (XPS) spectra were acquired with an ESCA Lab 250 (Thermo) spectrometer (Shanghai, China) using a monochromatic Al Ka source (1486.6 eV). The X-ray diffraction (XRD) patterns of the samples were recorded with a Rigaku D/max 2500 X-ray diffractometer (Dandong, China) using Cu $K\alpha$ radiation (30 kV, 25 mA) in the range $2\theta = 2°–80°$. The size and morphology of the nanoparticles were observed by scanning electron microscopy (SEM) using a Hitachi S4800 field emission electron microscope (Tokyo, Japan) operated at 30 kV and transmission electron microscopy (TEM) using a JEOL model JEM-2011(HR) (Tokyo, Japan) at 200 kV. The Brunauer–Emmett–Teller (BET) surface areas were determined from the N_2 adsorption at 77 K using V-Sorb 2800P (Jinaipu, China). The metal content of the materials was analyzed by a T.J.A. ICP-9000 type inductively coupled plasma atomic emission spectroscopy (ICP-AES) instrument. Gas chromatography (GC) analyses were carried out on an Agilent 7820A series gas chromatograph (Agilent Technologies, CA, USA) equipped with a flame ionization detector (FID) and a split/splitless injector. All the separations were performed on a HP-5 capillary column (30 m × 0.32 mm i.d. × 0.25 μm film thickness) (Agilent J&W Scientific, CA, USA). An Agilent 7820A gas chromatography-5977E mass spectrometry system (GC-MS) (Santa Clara, CA, USA) was employed to identify all reaction products.

2.3 Synthesis of NPC-UiO-66-T, NPC- Al-MOF-800, NPC-MIL-125-800, and ZrO_2

The UiO-66(NH_2) was prepared via a method as described[29] previously in a DMF–HCl mixed solvent with NH_2-BDC and $ZrCl_4$ as the organic linker and the metal source, respectively. In brief, NH_2-BDC (1.34 g, 7.5 mmol) was dissolved in 100 mL of DMF under ultrasonication for 10 min. Then the $ZrCl_4$ (1.25 g, 5.4 mmol) and 60 mL DMF:HCl (5:1, v/v) were added into the mixture and sonicated for 10 min. Subsequently, the solution was transferred to a 200 mL Teflon-lined stainless steel autoclave. The autoclave was sealed and heated in an oven at 80 ^{o}C overnight under autogenous pressure, and after cooling naturally, the sample was washed with methanol to make sure that the occluded DMF molecules were eliminated. The yellow UiO-66(NH_2) product was dried in a vacuum at 80 ^{o}C for 4 h. Then, the UiO-66(NH_2) was heated in a horizontal tube furnace at different temperatures (700 ^{o}C, 800 ^{o}C and 900 ^{o}C, respectively) for 3 h under a flow of nitrogen gas. The resulting product was denoted as NPC-UiO-66-T, where T represents the carbonization temperature (700 ^{o}C, 800 ^{o}C and 900 ^{o}C).

UiO-66 was prepared following a modified procedure as described in literature.[26] In a typical synthetic process, 106 mg of $ZrCl_4$ and 68 mg of BDC were dissolved in 50 mL DMF and sealed in a stainless steel vessel with Teflon liner. Then the solution was put into a preheated oven at 120 ^{o}C. After 48 h, the oven was naturally cooled to room temperature. The solid was filtered out, washed with DMF and absolute ethanol and then dried in air at 90 ^{o}C. UiO-66 was

View Article Online
DOI: 10.1039/C7NJ00442G

directly carbonized at 800 °C under a flow of nitrogen gas. The obtained solid was named as C-UiO-66-800. To preparation of the Zr-free-NPC-UiO-66-800, 50 mg of NPC-UiO-66-800 powder was dispersed in 20 mL of 50% H_2SO_4 and stirred at 80 °C for 6 h. Then the mixture was collected by centrifugation and washed with distilled water until the pH reached 7. Finally, the Zr-free-NPC-UiO-66-800 was obtained by vacuum drying at 60 °C for 5 h.

NH_2-Al-MOF was prepared according to the reported procedure.[30] $AlCl_3 \cdot 6H_2O$ (4.635 g, 19.2 mmol), NH_2-BDC (1.165 g, 6.45 mmol) and methanol (61.75 mL) were transferred into a 100 mL Teflon-lined stainless steel autoclave. Then the autoclave was heated to 125 °C for 5 h under autogenous pressure. After cooling, the precipitate was centrifuged and yellow microcrystalline solid was obtained. The microcrystalline product was washed with deionized water three times and dried at 80 °C under vacuum. The synthesis of NH_2-MIL-125(Ti) crystals was accomplished using a solvothermal route.[31] In a typical synthesis, NH_2-BDC (1.12 g, 6.2 mmol) was dissolved in 60 mL DMF and methanol mixed solvent ($V_{DMF}/V_{methanol}$ = 9:1). Then TPOT (1.2 mL, 4.0 mmol) was added to the solution. After stirring by ultrasonic concussion for 5 minutes, the mixture was transferred to a 100 mL Teflon-lined steel autoclave and the autoclave was placed in an oven at 150 °C for 24 h under static conditions. After cooling, the yellow solid product, NH_2-MIL-125(Ti), was washed three times with DMF and twice with methanol. Then it was dried overnight in a vacuum oven at 60 °C. NPC- MIL-125-800 and NPC-Al-MOF-800 was prepared according to the procedure for C-UiO-66-800 except that NH_2-MIL-125(Ti) and NH_2-Al-MOF was used.

ZrO_2 powders were prepared by a conventional precipitation method following the reported procedure.[32] Briefly, 12.9 g $ZrOCl_2 \cdot 8H_2O$ was dissolved in 200 mL deionized water at room temperature, and the pH was adjusted to about 9 by dropwise addition of NH_4OH (2.5 mol L^{-1}) under stirring. After stirring for 8 h, the resultant hydrogel was washed with deionized water until free of chloride ions. The precipitate was then dried at 110 °C overnight and calcined at 400 °C in air for 2 h.

2.4 Synthesis of supported AgPd catalysts

AgPd@NPC-UiO-66-T was prepared by the impregnation method. Typically, 95 mg of NPC-UiO-66-T, 7.5 mL H_2PdCl_4 solution (1 mg mL^{-1}) and 0.8 mL $AgNO_3$ solution (1 mg mL^{-1}) were added into a 25 mL round bottomed flask and ultrasonicated for 5 min, then the solution was stirred for 6 h at room temperature. Subsequently, 2 mL $NaBH_4$ (0.66 mol L^{-1}) solution was added dropwise and vigorous stirred for 2 h. The product was collected by centrifugation, washed with H_2O until the pH reached 7, and dried at 60 °C in vacuum oven to yield Ag_1Pd_9@NPC-UiO-66-800. Ag_2Pd_8@NPC-UiO-66-800, Ag_3Pd_7@NPC-UiO-66-800, Ag@NPC-UiO-66-800 and Pd@NPC-UiO-66-800 catalysts were synthesized with the above procedure except that the molar ratios of Ag and Pd were 2:8, 3:7, 10:0 and 0:10, respectively. The content of Ag and Pd in the composite was determined by ICP-AES (Table 1). Ag_1Pd_9@C-UiO-66-800, Ag_1Pd_9@Zr-free-NPC-UiO-66-800, Ag_1Pd_9@NPC-MIL-125-800 and Ag_1Pd_9@NPC-Al-MOF-800 were prepared with the above procedure except that C-UiO-66-800, Zr-free-NPC-UiO-66-800, NPC-MIL-125-800 and NPC-Al-MOF-800 were used, respectively. AgPd nanoparticles catalyst was fabricated with the above procedure without the addition of NPC-UiO-66-T.

Table 1 Amount of Ag and Pd in AgPd@NPC-UiO-66-800 catalysts.

Catalysts	Ag (wt%)	Pd (wt%)	Ag–Pd initial composition	Ag–Pd final composition
Ag_1Pd_9@NPC-UiO-66-800	0.49	4.39	1:9	1:8.96
Ag_2Pd_8@NPC-UiO-66-800	0.93	3.91	2:8	2:8.41
Ag_3Pd_7@NPC-UiO-66-800	1.39	3.37	3:7	3:7.27

2.5 Catalytic transfer hydrogenation of nitro compounds

Typically, to a mixture of nitro compound (1 mmol), catalyst (1 mol%), and 252 mg (4 mmol) ammonium formate in 5 mL methanol , 172 µL formic acid (4 mmol) was added and then the reaction mixture was stirred at 25 °C for a certain time. The reaction progress was monitored by thin layered chromatography. The yield of the product was analyzed by GC. After completion of the reaction, the recovered catalyst was separated by centrifugation and repeatedly washed with methanol to remove the organic and inorganic part and dried in vacuum at 60 °C overnight for another consecutive reaction run. The product was extracted with ethyl acetate (3×5 mL) and dried over anhydrous $MgSO_4$ and then evaporated under vacuum. The structure of the product was confirmed by GC-MS.

3. Results and Discussion

3.1 Characterization of the catalyst

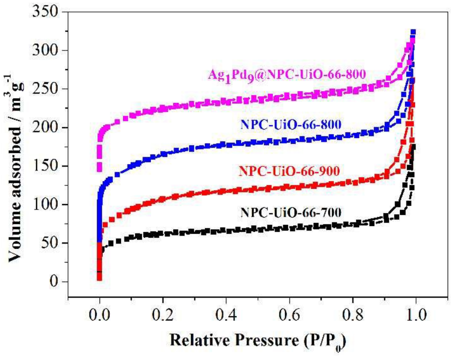

Fig 1. The nitrogen adsorption-desorption isotherms of NPC-UiO-66, Ag_1Pd_9@NPC-UiO-66-800.

The porosity of the NPC-UiO-66 and AgPd-NPC-UiO-66-800 was determined employing N_2 adsorption/desorption analysis at 77 K (Fig 1). The series of characterizations N_2 adsorption studies revealed that NPC-UiO-66 contained micropore, mesopore and a small amount of macropore. The surface areas and pore volumes of NPC-UiO-66 is related to the carbonization temperature, which are 210 m^2 g^{-1} and 0.27 m^3 g^{-1} for NPC-UiO-66-700, 417 m^2 g^{-1} and 0.43 m^3 g^{-1} for NPC-UiO-66-800, 371 m^2 g^{-1} and 0.39 m^3 g^{-1} for NPC-UiO-66-900, respectively. As shown in Fig 1, the Ag_1Pd_9-NPC-UiO-66-800 also showed similar characteristic with NPC-UiO-66. The BET surface area and pore volume of the Ag_1Pd_9@NPC-UiO-66-

View Article Online
DOI: 10.1039/C7NJ00442G

800 is 356 m^2 g^{-1} and 0.38 m^3 g^{-1}. The slightly decrease in the BET surface area suggests the occupation of AgPd NPs inside the nanoporous channel of the NPC-UiO-66. As shown in the TEM image (Fig 2) of Ag_1Pd_9@NPC-UiO-66-800, fine Pd NPs are uniformly distributed throughout the porous carbon (Fig 2A). The high-resolution TEM image displays clear lattice fringe, suggesting the good crystallinity. Besides, the lattice spacing is measured to be 0.23 nm, which is between the (111) plane of face-centered cubic (fcc) Pd (0.224 nm)[33] and fcc Ag (0.235 nm)[34], suggesting that AgPd is formed as an alloy structure, which is also supported by STEM-EDS line-scan of Ag_1Pd_9@NPC-UiO-66-800 (Fig S1) and the XRD results. Fig 3 shows the XRD patterns of the as-synthesized materials. The well-defined diffraction peak of Ag_1Pd_9, Ag_2Pd_8 and Ag_3Pd_7 NPs is between the peaks of Ag (2θ = 38.03°) and Pd (2θ = 40.10°) NPs, further indicating that AgPd is formed as an alloy. The diffraction lines at 2θ=28.4°, 31.5°, 50.6°, 60.3° were attributed to the monoclinic phase of the ZrO_2 support (m-ZrO_2), the tetragonal ZrO_2 (t-ZrO_2) was observed at 2θ = 30.17°, 34.3°, which is in good agreement with the standard cards (JCPDS PDF no. 37-1484 and JCPDS PDF no. 49-1642 respectively).[35] The results indicated the existence of both monoclinic and tetragonal mixed phase ZrO_2 in the support.

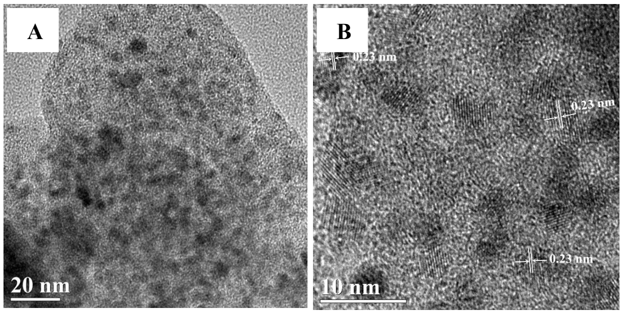

Fig 2. TEM pattern (A) and HRTEM pattern (B) of Ag_1Pd_9@NPC-UiO-66-800.

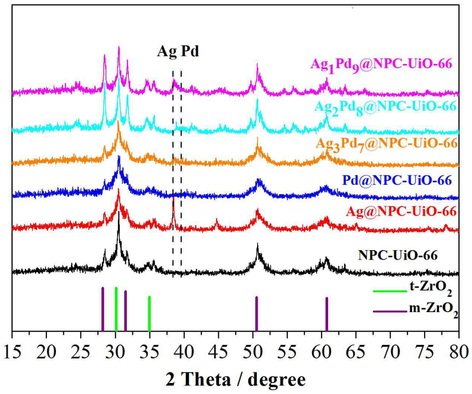

Fig 3. The XRD pattern of NPC-UiO-66, AgPd@NPC-UiO-66-T and ZrO_2.

X-ray photoelectron spectroscopy analysis (Fig 4, Fig S2) and energy-dispersive X-ray spectroscopy (EDX) (Fig S3) confirmed the co-existence of Ag, Pd, Zr, C, N and O in the Ag_1Pd_9@NPC-UiO-66-800 catalyst. The Pd XPS spectra (Fig 4A) demonstrated that the Pd_{3d} spectral peaks at binding energy 335.1 and 341.1 eV were dominant, which were attributed to Pd^0 and indicate that metallic Pd was formed as the major phase on the support. While in Fig 4C, the $3d_{3/2}$ peaks of Ag^0 appear at 373.4 and 374.9, the $3d_{5/2}$ peak of Ag^0 appear at 367.9 eV, respectively, with no obvious peak of Ag^+ was observed, indicating the co-existence of both metals. Besides, XPS results showed that both Ag and Pd are in the reduced states. Compared to the monometallic Pd@NPC-UiO-66-800 and Ag@NPC-UiO-66-800 samples, the 3d peaks for Ag(0) and Pd(0) in Ag_1Pd_9@NPC-UiO-66-800 shift to lower binding energies by ~0.8 and~0.5 eV, respectively (Fig S4). Such observed shifts for both Pd 3d and Ag 3d may be attributed to the flow of electron from Ag to Pd (gaining electrons from Ag), indicative of the presence of an interaction between Ag and Pd and the formation of AgPd alloy NPs, which is in good agreement with previous reports.[36] The formation of AgPd alloy NPs is reasonable because the two soluble metal salts have close reduction potentials ($E°_{Ag^+/Ag}$ = +0.80 eV vs SHE; $E°_{Pd^{2+}/Pd}$ = +0.915 eV vs SHE, SHE: standard hydrogen electrode). Besides, the line scan results unambiguously demonstrated that Ag-Pd was formed as an alloy structure (Fig S1). Two Zr $3p_{3/2}$ and Zr $3p_{1/2}$ peaks were identified at approximately 332.5 and 346.5 eV (Fig 4A), respectively, and these two binding energies in particular indicated the presence of ZrO_2. In Fig 4B, the characteristic peaks for oxidation state of Zr can be clearly seen at 182.2 and 184.5 eV assigned to Zr $3d_{5/2}$ and Zr $3d_{3/2}$, respectively, revealing that ZrO_2 was present in the catalyst. The surface nitrogen content estimated from the XPS data was ~2 wt. %. The *N*1s XPS spectrum (Fig 4D) could be fitted well to peak positioned at binding energy of 400.0 eV.

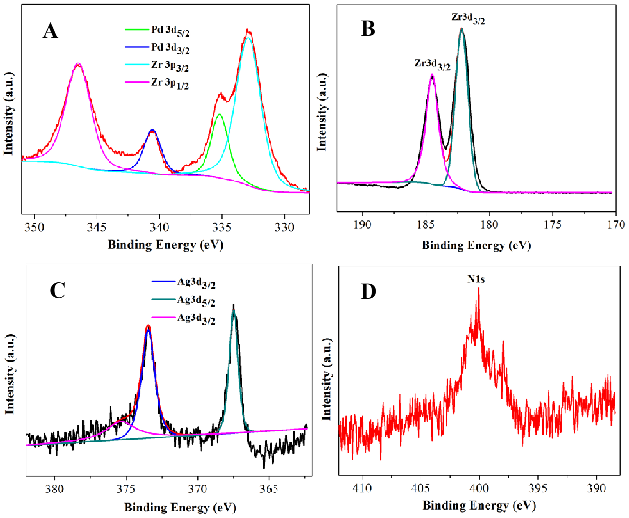

Fig 4. The XPS images of Pd (A), Zr (B), Ag (C) and N (D) of Ag_1Pd_9@NPC-UiO-66-800.

3.2 The catalytic hydrogenation of nitroarenes

At the start of our work, the reduction of nitrobenzene was investigated as a benchmark system to development an optimal catalytic system, various reaction parameters such as the type of catalysts, hydrogen sources, solvent, catalyst dosage were optimized. We started our study with CTH of nitrobenzene in

View Article Online
DOI: 10.1039/C7NJ00442G

methanol catalyzed by Ag_1Pd_9@NPC-UiO-66-800 (1 mol%) at 25 ^{o}C with different hydrogen sources. Only 15% aniline was obtained after 12 h when we employed FA as the hydrogen source (Table S1, entry 1). In contrast to the protocols reported previously,[37] the addition of formate in the catalytic system can significantly enhance the reaction efficiency. Among the hydrogen donor investigated, the excellent result was achieved when 1:1 (molar ratio) FA/AF was employed (Table S1, entries 2-6). Aniline was obtained in a high yield of 99% with excellent selectivity at 25 ^{o}C for 20 min. Relative long reaction time was required when 1:1 FA/HCOONa, or FA/HCOOK were used as the hydrogen source. In the blank experiment, no reaction occurred in the absence of catalyst, using NPC-UiO-66-800 or ZrO_2 as the catalyst at room temperature (Table 2, entries 1-3), suggesting that integrated AgPd NPs play a decisive role in catalyzing the CTH reaction.

A further noteworthy finding in the present work is that apart from the AgPd NPs, the component of the underlying support also plays an essential role in determining the catalytic performance of the final materials. For comparison, the hydrogenation of nitrobenzene over Ag_1Pd_9@Zr-free-NPC-UiO-66-800 was investigated (Table 2, entry 5). Triple reaction time is required in the absence of ZrO_2. Compared with Ag_1Pd_9@Zr-free-NPC-UiO-66-800, Ag_1Pd_9@NPC-UiO-66-800 exhibited much higher activity revealing that ZrO_2 also play very important role for the CTH of nitroarenes. Previous researches have demonstrated that nitro groups can be easily adsorbed on the basic or reducible supports.[38, 39] Zirconia is weakly basic and possesses redox functions, which may forebode a strong interaction between ZrO_2 surface and nitro groups.[40]

To further examine the effect of metal oxide on the catalytic activity of the catalyst, Ag_1Pd_9@NPC-Al-MOF and Ag_1Pd_9@NPC-MIL-125, in which containing Al_2O_3 and TiO_2 respectively, were prepared and their catalytic activity was evaluated at the identical reaction conditions (Table 2, entries 6, 7). The conversions of nitrobenzene were 52% and 99% at 60 min for the Ag_1Pd_9@NPC-Al-MOF and Ag_1Pd_9@NPC-MIL-125 catalysts, respectively. These results indicated that both the noble metal and the nature of the support played important roles in the CTH of nitroarenes. The previous study has demonstrated that the zirconia support can substantially facilitate crucial FA deprotonation,[41] thus achieve FA dehydrogenation efficiently. We can say it specifically that the combination of AgPd NPs and NPC-UiO-66 containing ZrO_2 is found to be crucial to give an exceptionally active catalyst capable of facilitating the CTH of nitro compounds under ambient conditions.

To illustrate the role of nitrogen in the catalyst, the hydrogenation of nitrobenzene over nitrogen-free Ag_1Pd_9@C-UiO-66-800 catalyst was investigated (Table 2, entry 8). Compared with Ag_1Pd_9@NPC-UiO-66-800, Ag_1Pd_9@C-UiO-66-800 exhibited lower catalytic activity and comparable selectivity. After 40 min reaction, the conversions of nitrobenzene were 99%. The result can be ascribed to that nitrogen doped support can affected the dispersion of metal nanoparticles, which can improve the catalytic activity for the transfer hydrogenation of nitrobenzene. This has been demonstrated by the previous reports.[15, 42] Bulusheva et al.[42] recently proposed that single isolated Pd atoms supported on *N*-doped carbon is an efficient catalyst for dehydrogenation from FA. *N*-doped graphene-Fe_2O_3 exhibited high catalytic performance for the hydrogenation of nitroarenes.[15] To further investigate whether the support has a dramatic effect on the catalytic activity of Ag_1Pd_9@NPC-UiO-66-800 hybrid, the catalytic activity of the AgPd NPs is also examined (Table 2, entries 9). It shows much lower catalytic activity than that of the Ag_1Pd_9@NPC-UiO-66-800 hybrid under analogous conditions.

Table 2 Reduction of nitrobenzene to aniline under various conditions. [a]

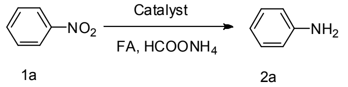

Entry	Cat	Solvents	Time (min)	Conversion (%)	Selectivity (%)
1	-	Methanol	6 h	-	-
2	NPC-UiO-66-800	Methanol	30 h	-	-
3	ZrO_2	Methanol	6 h	-	-
4	Ag_1Pd_9@NPC-UiO-66-800	Methanol	20	>99	>99
5	Ag_1Pd_9@Zr-free-NPC-UiO-66-800	Methanol	60	>99	>99
6	Ag_1Pd_9@NPC-Al-MOF	Methanol	60	52	83
7	Ag_1Pd_9@NPC-MIL-125	Methanol	60	>99	97
8	Ag_1Pd_9@C-UiO-66-800	Methanol	40	>99	98
9[b]	AgPd	Methanol	75	>99	>99
10	Ag@NPC-UiO-66-800	Methanol	6 h	-	-
11	Pd@NPC-UiO-66-800	Methanol	6 h	15	>99
12	Ag_2Pd_8@NPC-UiO-66-800	Methanol	60	>99	>99
13	Ag_3Pd_7@NPC-UiO-66-800	Methanol	2.5 h	>99	>99
14	Ag_1Pd_9@NPC-UiO-66-800	Water	2 h	45	>99
15	Ag_1Pd_9@NPC-UiO-66-800	DMF	2 h	98	>99
16	Ag_1Pd_9@NPC-UiO-66-800	Toluene	2 h	>99	95
17	Ag_1Pd_9@NPC-UiO-66-700	Methanol	70	>99	>99
18	Ag_1Pd_9@NPC-UiO-66-900	Methanol	30	>99	>99
19	Pd@C	Methanol	24 h	46	99
20[c]	Ag_1Pd_9@NPC-UiO-66-800	Methanol	3 h	>99	>99
21[d]	Ag_1Pd_9@NPC-UiO-66-800	Methanol	20 h	96	>99
22[e]	Ag_1Pd_9@NPC-UiO-66-800	Methanol	20	96	99

View Article Online
DOI: 10.1039/C7NJ00442G

[a] nitrobenzene (1 mmol), FA (4 mmol), $HCOONH_4$ (4 mmol), catalyst (1 mol% metal), solvent (5 mL); GC analysis using *n*-decane as an internal standard. [b] 1 mol% metal. [c] 0.5 mol% metal. [d] 0.1 mol% metal. [e] 10 mmol nitrobenzene.

An array of different catalysts, i.e., Ag@NPC-UiO-66-800, Pd@NPC-UiO-66-800 and AgPd@NPC-UiO-66-800 with different molar ratio of Ag and Pd were screened for the transfer hydrogenation reaction to determine the effect of the metal composition on the catalytic performance. No product was obtained in the absence of catalyst (Table 2, entry 1) indicating that the catalyst was necessary for the CTH reaction. Using NPC-UiO-66-800 and Ag@NPC-UiO-66-800 as catalyst (Table 2, entries 2, 10), no conversion of nitrobenzene was observed after 6 h. In addition, low nitrobenzene conversion of 15% was produced after 6 h in the presence of Pd@NPC-UiO-66-800 catalyst. To our surprise, bimetallic AgPd NPs catalyst, Ag_1Pd_9@NPC-UiO-66-800, exhibited excellent catalytic activity for the CTH of nitrobenzene. 99% of conversion and 99% of selectivity were achieved after 20 min reaction at 25 °C. Thus, it can be safely concluded that AgPd NPs were the catalytic active sites for the CTH of nitrobenzene and the cooperative effect between Ag and Pd plays a crucial role for realizing the highly catalytic performance of the catalyst. To further examine the effect of the ratio of Ag and Pd on the catalytic activity, Ag_2Pd_8@NPC-UiO-66-800 and Ag_3Pd_7@NPC-UiO-66-800 were fabricated. The results indicated that the catalytic activity decreased with increasing the ratio of Ag in AgPd@NPC-UiO-66-800 (Table 2, entries 12, 13), the reaction time needed 60 min and 2.5 h, respectively, to achieve 99% conversion.

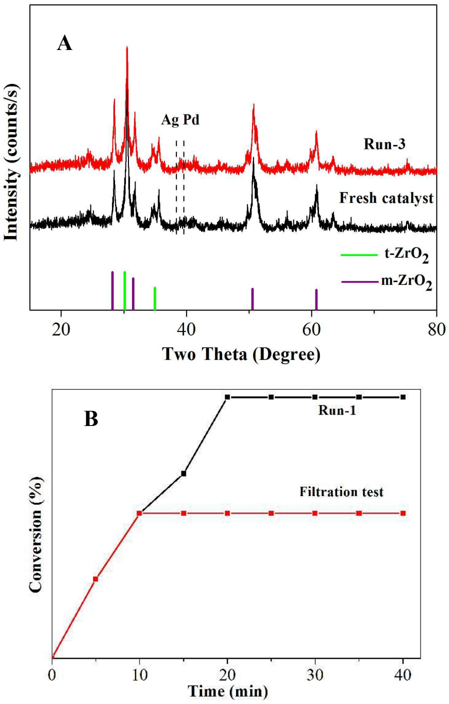

Fig 5. XRD pattern of Ag_1Pd_9@NPC-UiO-66-800 and ZrO_2 (A) and the filtration test for the reduction of nitrobenzene over Ag_1Pd_9@NPC-UiO-66-800 (B).

The effect of reaction solvent on the CTH reaction was also investigated. Using toluene, water and DMF as the solvent, the desired product was obtained in moderate or good conversions after 2 h reaction (Table 2, entries 14-16). We were pleased to find that the reaction occurred efficiently to afford the corresponding product after 20 min in 99% conversion and selectivity with methanol as the solvent (Table 2, entry 4). The effect of the dosage of catalyst was also investigated. When the Ag_1Pd_9@NPC-UiO-66-800 catalyst dosage was reduced from 1 mol% to 0.5 and 0.1 mol%, the reaction time needed 3 h and 20 h, respectively, to achieve complete conversion (Table 2, entries 20, 21). It is worth noting that the transfer hydrogenation of nitrobenzene catalyzed by Ag_1Pd_9@NPC-UiO-66-800 was performed in the air and it did not require conducting under nitrogen atmosphere. Therefore, the protocol of the catalytic transfer hydrogenation of nitro compounds is facile. Moreover, the newly developed methodology is also effective for the large scale reaction with consistent product conversion (Table 2, entry 22).

In order to evaluate the efficiency of the Ag_1Pd_9@NPC-UiO-66-800 for the transfer hydrogenation of nitrobenzene, the present catalytic system was compared with other reported catalysts in terms of the reaction temperature, reaction time and turnover frequency (TOF) (Table S2). The data in Table S2 indicated that the as-prepared Ag_1Pd_9@NPC-UiO-66-800 can efficiently catalyze the CTH reaction at mild conditions with high TOF.

The catalytic stability is also a very important criterion to evaluate the catalysts. A series of recycling experiments were conducted for the transfer hydrogenation of nitrobenzene under the same reaction condition to evidence the robustness and recyclability of the catalyst. The Ag_1Pd_9@NPC-UiO-66-800 can be easily recovered by centrifugation and reused up to five cycles. It can be seen that the activity and selectivity of Ag_1Pd_9@NPC-UiO-66-800 were well retained during five consecutive runs (Table S3), which demonstrated its recyclability. From the TEM image of the recycled catalyst, we can see that the AgPd NPs remain a high level of dispersion and crystallinity, which revealed the good stability of the catalyst (Fig S5). In addition, XRD results indicated that no obvious diffraction peak change can be observed between fresh and recycled catalyst (Fig 5A). The XPS spectra of the used catalyst (Fig S6) demonstrated that the existential states of Ag and Pd have not obvious difference with that of the fresh catalyst. In order to further confirm that the reduction of nitrobenzene is a real heterogeneous process, a filtration test was carried out after 10 min of the reaction. No further conversion was observed even after 2 h of reaction under identical conditions (Fig 5B). In addition, ICP-AES analysis indicated that no metal could be detected in the liquid solution. Since nitrogen is powerfully electronegative and usually has a lone pair of electrons, the nitrogen functionalities on the surface might act as Lewis base sites and are expected to be more effective in retaining metal NPs.[43] According to the above results, it can be safely concluded that the Ag_1Pd_9@NPC-UiO-66-800 catalyst was robust, recyclable and has great application potential in the catalytic reduction of nitro compounds.

To demonstrate the general applicability of this catalyst system, various substituted nitro compounds were investigated under the optimized conditions (Table 3).

View Article Online
DOI: 10.1039/C7NJ00442G

Table 3 Reduction of nitro compounds to corresponding amines. [a]

$$R{-}NO_2 \xrightarrow[\text{Methanol, 25 °C}]{\text{Cat, FA, HCOONH}_4} R{-}NH_2$$

Entry	Substrate	Product	Time (min)	Conversion (%)	Selectivity (%)	TOF [h^{-1}] [b]	TON[c]
1	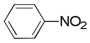	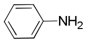	20	>99	>99	300	100
2	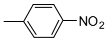	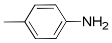	20	>99	>99	300	100
3	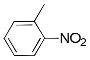	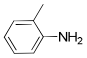	30	98	>99	196	98
4	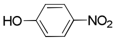	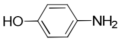	20	>99	>99	300	100
5	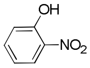	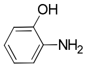	20	>99	>99	300	100
6	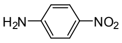	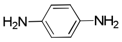	20	>99	>99	300	100
7	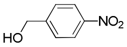	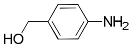	20	>99	>99	300	100
8	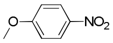	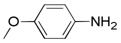	20	>99	>99	300	100
9	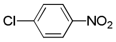	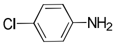	30	>99	98	200	100
10	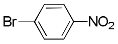	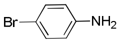	30	>99	97	194	97
11	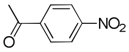	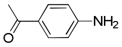	20	>99	>99	300	100
12	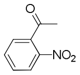	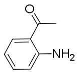	5 h	96	>99	19.2	96
13	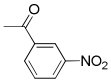	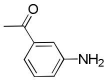	60	96	>99	96	96
14	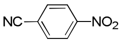	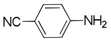	60	>99	>99	100	100
15	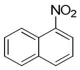	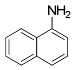	6 h	98	>99	16.3	98
16[d]	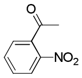	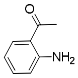	30	97	>99	194	97
17[d]	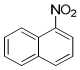	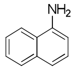	2 h	98	>99	49	98
18	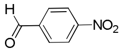	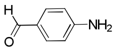	6 h	>99	>94	15.7	94

View Article Online
DOI: 10.1039/C7NJ00442G

19	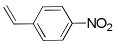	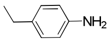	60	>99	>95	95	95
20	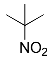	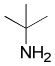	60	>99	>99	100	100

[a] Substrate (1 mmol), FA (4 mmol), $HCOONH_4$ (4 mmol), Ag_1Pd_9@NPC-UiO-66-800 (1 mol%), methanol (5 mL), 25 °C; GC analysis using *n*-decane as an internal standard. [b] turnover frequency: mol of substrate transformed per mol of catalyst per hour. [c] turnover number. [d] 50 °C.

The reaction was carried out in methanol at room temperature. Alkyl-substituted nitroarenes are reduced rapidly in excellent yields up to 99% (Table 3, entries 2, 3). Moreover, the nitro compounds involving electron-rich groups such as *o*-hydroxyl, *p*-hydroxyl, *p*-amino, *p*-methylol and *p*-methoxy were reduced to corresponding amine products in an efficient fashion with absolute selectivity (Table 3, entries 4-8). More importantly, for halogenated nitroarenes, full conversion is achieved (Table 3, entries 9, 10) and no dehalogenation product was obtained. Particularly, the nitroarenes functionalized with the most challenging reducible functional moieties, such as aldehydes, ketone and nitrile groups, were successfully transformed into corresponding amines products with an excellent selectivity (Table 3, entries 11-14, 18). The transfer hydrogenation of *o*-nitroacetophenone over the catalyst needed longer time to gain full conversion (Table 3, entry 12), which revealing slight space steric hindrance to the hydrogenation of the nitro group can be well tolerated. When the reaction temperature rose to 50 °C, the reaction time for hydrogenation of *o*-nitroacetophenone and 1-nitronaphthalene greatly decreased (Table 3, entries 16, 17), and the TOF were greatly raised. Next, the reduction of 4-nitrostyrene, which has both olefin and nitro moieties (Table 3, entry 19) [44], was investigated using Ag_1Pd_9@NPC-UiO-66-800 catalyst. Under the optimal reaction conditions, 4-nitrostyrene was converted to the completely reduced product 4-ethylaniline. To our delight, the reaction can be further extended to simple aliphatic nitro compounds, which was converted to the related primary amines with high yield in 1 h (Table 3, entry 20).

The influence of the substituents on the reduction rate of nitrobenzenes is represented by the Hammett $\sigma\rho$ -relationship :

$$\log\frac{k}{k_0} = \sigma\rho$$

where k is the rate constant of the catalytic reduction of substituted nitrobenzenes and k_0 indicates the rate constant of the unsubstituted nitrobenzene. The k-values were evaluated from the initial reduction rates. [45] The corresponding Hammett plot (Fig. S7) reveals that the rate of reaction is decreased by electron donating groups and enhanced by electron attracting substituents. The resulting slope (ρ) of the $\sigma\rho$–relationship obtained by linear regression is 0.347 (correlation coefficient: r^2=0.961), indicative of an anionic charge on the transition state.

According to the precious works, a schematic mechanism was proposed for the CTH of nitro compounds over the Ag_1Pd_9@NPC-UiO-66-800 catalyst. As shown in Fig S8, nitrobenzene firstly absorbs on the surfaces of the catalyst. The activation of FA and AF by AgPd NPs would generate active AgPd-H species, which were used for the hydrogenation of nitrobenzene to amines. Finally, the product amines release from the surface of the Ag_1Pd_9@NPC-UiO-66-800 catalyst. Then, the next catalytic cycle is started.

4. Conclusions

In summary, bimetallic AgPd nanoparticles supported on *N*-doped porous carbon have been successfully fabricated. With FA and AF as the hydrogen donor, the as-prepared Ag_1Pd_9@NPC-UiO-66-800 catalyst exhibited high activity for the catalytic transfer hydrogenation of substituted nitroarenes at room temperature. The superior catalytic performance can be attributed to the synergistic effect between the highly dispersed AgPd NPs and unique structure of NPC-UiO-66 support, as well as the high adsorption ability of the catalyst for the nitroarenes. The approach in this work can be potentially used to develop novel efficient catalysts for hydrogenations in the future.

Acknowledgements

Financial supports from the National Natural Science Foundation of China (21603054), the Natural Science Foundation of Hebei Province (B2015204003, B2016204131), the Young Top-notch Talents Foundation of Hebei Provincial Universities (BJ2016027), and the Natural Science Foundation of Agricultural University of Hebei (ZD201506, ZD201613) are gratefully acknowledged.

Notes and references

College of Science
Agricultural University of Hebei
Baoding 071001, Hebei Province, P. R. China
Fax: (+86)312-7528292
E-mail: chunwang69@126.com (C. Wang);
fengchengcctv@163.com (C. Feng)

Electronic Supplementary Information (ESI) available: Reduction of nitrobenzene to aniline with different hydrogen source over Ag_1Pd_9@NPC-UiO-66-800 catalyst. Various reported catalyst tested for reduction of nitroarenes into anilines. EDX spectrum, XPS patterns and recyclability of the catalyst. TEM and XPS of the reused of the catalyst. Tentative reaction mechanism for the reduction of nitroarenes over the catalyst. See DOI: 10.1039/b000000x/

1. L. Liu, P. Concepción and A. Corma, *J. Catal.*, 2016, **340**, 1-9.
2. Y. Liu, Y. Lu, M. Prashad, O. Repi and T. J. Blacklock, *Adv. Synth. Catal.*, 2005, **347**, 217-219.
3. Y. B. Huang, Q. Wang, J. Liang, X. Wang and R. Cao, *J. Am. Chem. Soc.*, 2016, **138**, 10104-10107.

View Article Online
DOI: 10.1039/C7NJ00442G

4. Q. Yang, P. Q. Xu, S. H. Yu and H. L. Jiang, *Angew. Chem. Int. Ed.*, 2016, **55**.
5. M. J. Gilkey and B. Xu, *ACS Catal.*, 2016, **6**, 1420-1436.
6. K. J. Datta, A. K. Rathi, M. B. Gawande, V. Ranc, G. Zoppellaro, R. S. Varma and R. Zboril, *ChemCatChem*, 2016, **8**, 2351-2355.
7. J.-w. Zhang, G.-p. Lu and C. Cai, *Catal. Commun.*, 2016, **84**, 25-29.
8. S. Byun, Y. Song and B. M. Kim, *ACS Appl. Mater. Int.*, 2016, **8**, 14637-14647.
9. P. Zhou, D. Li, S. Jin, S. Chen and Z. Zhang, *Int. J. Hydrogen Energy*, 2016, **41**, 15218-15224.
10. J. Feng, C. Yang, D. Zhang, J. Wang, H. Fu, H. Chen and X. Li, *Appl. Catal. A: Gen.*, 2009, **354**, 38-43.
11. H. Heeres, R. Handana, D. Chunai, C. Borromeus Rasrendra, B. Girisuta and H. Jan Heeres, *Green Chem.*, 2009, **11**, 1247.
12. J. Mondal, Q. T. Trinh, A. Jana, W. K. Ng, P. Borah, H. Hirao and Y. Zhao, *ACS Appl. Mater. Int.*, 2016, **8**, 15307-15319.
13. L. Yu, Q. Zhang, S. S. Li, J. Huang, Y. M. Liu, H. Y. He and Y. Cao, *ChemSusChem*, 2015, **8**, 3029-3035.
14. I. Sorribes, G. Wienhofer, C. Vicent, K. Junge, R. Llusar and M. Beller, *Angew. Chem. Int. Ed.*, 2012, **51**, 7794-7798.
15. R. V. Jagadeesh, K. Natte, H. Junge and M. Beller, *ACS Catal.*, 2015, **5**, 1526-1529.
16. Y.-B. Huang, M. Shen, X. Wang, P.-C. Shi, H. Li and R. Cao, *J. Catal.*, 2015, **330**, 452-457.
17. H. C. Zhou and S. Kitagawa, *Chem. Soc. Rev.*, 2014, **43**, 5415-5418.
18. Y. B. Huang, J. Liang, X. S. Wang and R. Cao, *Chem. Soc. Rev.*, 2017, **46**, 126-157.
19. H. L. Jiang, B. Liu, Y. Q. Lan, K. Kuratani, T. Akita, H. Shioyama, F. Zong and Q. Xu, *J. Am. Chem. Soc.*, 2011, **133**, 11854-11857.
20. Y.-Z. Chen, C. Wang, Z.-Y. Wu, Y. Xiong, Q. Xu, S.-H. Yu and H.-L. Jiang, *Adv. Mater.*, 2015, **27**, 5010-5016.
21. L. Zhang, C. Feng, S. Gao, Z. Wang and C. Wang, *Catal. Commun.*, 2015, **61**, 21-25.
22. Y. Li, Y. X. Zhou, X. Ma and H. L. Jiang, *Chem. Commun.*, 2016, **52**, 4199-4202.
23. C. Feng, Y. Wang, S. Gao, N. Shang and C. Wang, *Catal. Commun.*, 2016, **78**, 17-21.
24. Y. Z. Chen, C. Wang, Z. Y. Wu, Y. Xiong, Q. Xu, S. H. Yu and H. L. Jiang, *Adv. Mater.*, 2015, **27**, 5010-5016.
25. Y. Luan, Y. Qi, H. Gao, N. Zheng and G. Wang, *J. Mater. Chem. A*, 2014, **2**, 20588-20596.
26. C. S. Hinde, W. R. Webb, B. K. Chew, H. R. Tan, W. H. Zhang, T. S. Hor and R. Raja, *Chem. Comm.*, 2016, **52**, 6557-6560.
27. Z. Xu, L. Yang and C. Xu, *Anal. Chem.*, 2015, **87**, 3438-3444.
28. S.-T. Gao, W. Liu, C. Feng, N.-Z. Shang and C. Wang, *Catal. Sci. Technol.*, 2016, **6**, 869-874.
29. M. J. Katz, Z. J. Brown, Y. J. Colon, P. W. Siu, K. A. Scheidt, R. Q. Snurr, J. T. Hupp and O. K. Farha, *Chem. Commun.*, 2013, **49**, 9449-9451.
30. T. Ahnfeldt, N. Guillou, D. Gunzelmann, I. Margiolaki, T. Loiseau, G. Ferey, J. Senker and N. Stock, *Angew. Chem. Int. Ed.*, 2009, **48**, 5163-5166.
31. S. Hu, M. Liu, K. Li, Y. Zuo, A. Zhang, C. Song, G. Zhang and X. Guo, *CrystEngComm*, 2014, **16**, 9645-9650.
32. X. L. Du, L. He, S. Zhao, Y. M. Liu, Y. Cao, H. Y. He and K. N. Fan, *Angew. Chem. Int. Ed.*, 2011, **50**, 7815-7819.
33. Y. Xiong, J. M. McLellan, Y. Yin and Y. Xia, *Angew. Chem. Int. Ed.*, 2007, **46**, 790-794.
34. Y. Ping, J.-M. Yan, Z.-L. Wang, H.-L. Wang and Q. Jiang, *J. Mater. Chem. A*, 2013, **1**, 12188.
35. K. Gurushantha, K. S. Anantharaju, L. Renuka, S. C. Sharma, H. P. Nagaswarupa, S. C. Prashantha, Y. S. Vidya and H. Nagabhushana, *RSC Adv.*, 2017, **7**, 12690-12703.
36. Y.-Z. Chen, Y.-X. Zhou, H. Wang, J. Lu, T. Uchida, Q. Xu, S.-H. Yu and H.-L. Jiang, *ACS Catal.*, 2015, **5**, 2062-2069.
37. G. Wienhofer, I. Sorribes, A. Boddien, F. Westerhaus, K. Junge, H. Junge, R. Llusar and M. Beller, *J. Am. Chem. Soc.*, 2011, **133**, 12875-12879.
38. A. Corma, P. Serna and H. García, *J. Am. Chem. Soc.*, 2007, **129**, 6358-6359.
39. M. Boronat, P. Concepción, A. Corma, S. González, F. Illas and P. Serna, *J. Am. Chem. Soc.*, 2007, **129**, 16230-16237.
40. G. Postole, B. Chowdhury, B. Karmakar, K. Pinki, J. Banerji and A. Auroux, *J. Catal.*, 2010, **269**, 110-121.
41. Q. Y. Bi, X. L. Du, Y. M. Liu, Y. Cao, H. Y. He and K. N. Fan, *J. Am. Chem. Soc.*, 2012, **134**, 8926-8933.
42. D. A. Bulushev, M. Zacharska, A. S. Lisitsyn, O. Y. Podyacheva, F. S. Hage, Q. M. Ramasse, U. Bangert and L. G. Bulusheva, *ACS Catal.*, 2016, **6**, 3442-3451.
43. X. Xu, Y. Li, Y. Gong, P. Zhang, H. Li and Y. Wang, *J. Am. Chem. Soc.*, 2012, **134**, 16987-16990.
44. A. Corma and P. Serna, *Science*, 2006, **313**, 332-334.
45. M. Lauwiner, P. Rys and J. Wissmann, *Appl. Catal., A*, 1998, **172**, 141–148.

View Article Online
DOI: 10.1039/C7NJ00442G

High catalytic activity of bimetallic AgPd alloy supported on UiO-66 derived porous carbon for transfer hydrogenation of nitroarenes using formic acid-formate as hydrogen source

Saisai Cheng, Ningzhao Shang, Xin Zhou, Cheng Feng*, Shutao Gao, Chun Wang*[a], Zhi Wang

College of Science, Hebei Agricultural University, Baoding 071001, China

Bimetallic AgPd nanoparticles supported on metal-organic framework (UiO-66) derived N-doped porous carbon (NPC-UiO-66). The as-synthesized Ag_1Pd_9@NPC-UiO-66 catalyst exhibited extraordinary catalytic activity toward the hydrogenation of nitroarenes to anilines at room temperature.